Available online at www.sciencedirect.com

SciVerse ScienceDirect

Journal of the European Ceramic Society 32 (2012) 891–898

www.elsevier.com/locate/jeurceramsoc

Composition and poling condition-induced electrical behavior of $(Ba_{0.85}Ca_{0.15})(Ti_{1-x}Zr_x)O_3$ lead-free piezoelectric ceramics

Jiagang Wu [a,*], Dingquan Xiao [a], Wenjuan Wu [a], Qiang Chen [a], Jianguo Zhu [a], Zhengchun Yang [b], John Wang [b]

[a] *Department of Materials Science, Sichuan University, Chengdu 610064, PR China*
[b] *Department of Materials Science and Engineering, National University of Singapore, Singapore 117574, Singapore*

Received 21 July 2011; received in revised form 31 October 2011; accepted 1 November 2011
Available online 3 December 2011

Abstract

Lead-free $(Ba_{0.85}Ca_{0.15})(Ti_{1-x}Zr_x)O_3$ (BCTZ) piezoelectric ceramics were fabricated by normal sintering in air atmosphere. BCTZ ceramics with $x = 0.10$ possess a coexistence of tetragonal and rhombohedral phases at ~40 °C. The Curie temperature of BCTZ ceramics decreases with increasing the Zr content. Piezoelectric properties of BCTZ ceramics are dependent on the poling conditions (i.e., the poling temperature and the poling electric field), and the underlying physical mechanism is illuminated by the phase angle. The BCTZ ($x = 0.10$) ceramic, which locates at the existence of two phases and is poled at $E \sim 4.0$ kV/mm and $T_p \sim 40$ °C, exhibits an optimum electrical behavior at a room temperature of ~20 °C: $d_{33} \sim 423$ pC/N, $k_p \sim 51.2\%$, $2P_r \sim 18.86\ \mu C/cm^2$, $2E_c \sim 0.47$ kV/mm, $\varepsilon_r \sim 2892$, and $\tan\delta \sim 1.53\%$.

Keywords: Lead-free ceramics; Piezoelectric properties

1. Introduction

Lead-free piezoelectric materials have been recently given to much attention due to their high piezoelectric properties, environmental friendliness, etc., promising as the candidate materials for buzzers, transducers, and piezoelectric transformers.[1–4] Among those, most interests have focused on the relationship between phase structure and electrical behavior of $K_{0.50}Na_{0.50}NbO_3$ and $Bi_{0.5}Na_{0.5}TiO_3$-based piezoelectric ceramics.[1–13] Ren et al.[7] have recently reported that a high piezoelectric constant (d_{33}) superior to PZT materials is well established for the ion-modified $BaTiO_3$ ceramics by constructing a tricritical point at room temperature. Damjanovic[10] thought that the polarization rotation and polarization extension should be responsible for the enhancement of their electrical properties. Therefore, it is worth further exploring the relationship between phase structure and electric behavior of $BaTiO_3$-based ceramics for practical applications.

Some attempts have been conducted to improve the d_{33} value of lead-free piezoelectric ceramics, such as by the employment of the template grain growth,[1] the site engineering,[5–7,13] the introduction of sintering aids,[14] and the construction of the coexistence of two or more phases.[5,6,13,15,16] Among those, a composition-induced phase transition is a very promising method to achieving a higher piezoelectricity for lead-free piezoelectric ceramics,[5,6,13,15] where the polarization direction at the phase transition can be easily rotated with applied electric fields, owing to the instability of the polarization state.[17–19] The phase boundary among three phases of BCTZ ceramics is not vertical and shows a strong temperature dependence.[9] Therefore, it is important to investigate the effect of the poling condition (i.e., poling temperature and poling electric field) on the piezoelectric properties of BCTZ ceramics, where there are few systematic reports on it for BCTZ ceramics.

In this work, the $(Ba_{0.85}Ca_{0.15})(Ti_{1-x}Zr_x)O_3$ (BCTZ) lead-free piezoelectric ceramics were fabricated by the conventional ceramic processing, whereas all ceramics were sintered in air

* Corresponding author.
E-mail addresses: wujiagang0208@163.com, msewujg@scu.edu.cn (J. Wu).

0955-2219/$ – see front matter © 2011 Elsevier Ltd. All rights reserved.
doi:10.1016/j.jeurceramsoc.2011.11.003

atmosphere. The relationship between phase structure and electrical properties of BCTZ ceramics is discussed, the effect of the poling condition on the piezoelectric properties of BCTZ ceramics is also investigated, and the underlying physical mechanisms are addressed.

2. Experimental procedure

$(Ba_{0.85}Ca_{0.15})(Ti_{1-x}Zr_x)O_3$ ($x = 0$, 0.05, 0.075, 0.09, 0.10, 0.11, 0.125, 0.15, and 0.20) ceramics were prepared by the normal sintering. $BaCO_3$ (99.9%, Alfa Aesar), $CaCO_3$ (99%, Alfa Aesar), TiO_2 (99%, Alfa Aesar), and ZrO_2 (99%, Alfa Aesar) were used as starting raw materials. They were ball milled for 24 h with agate ball media and alcohol. After calcination at 1200 °C for 3 h, the calcined powders were milled again for 12 h, and pressed into the disks of ~1.5 cm diameter and ~1.0 mm thickness under 20 MPa using PVA as a binder. After burning off PVA, the pellets were sintered at 1500 °C for 2 h in air. Gold paste was sintered on both sides of samples at ~700 °C for 20 min to form the electrodes for their electrical measurements. The ceramics are poled in a 20–90 °C silicon oil bath by applying the *dc* electric fields for 30 min. All measurement of electrical properties is conducted after 24 h.

The phases present in these ceramics were analyzed by using X-ray diffraction (Bruker D8 Advanced XRD, Bruker AXS Inc., Madison, WI, CuKa). The high temperature XRD and Raman spectroscopy were used to confirm the phase transition of these ceramics. Scanning electron microscopy (SEM) (Philips, XL30) was employed to study the surface morphologies of these ceramics. The piezoelectric constant d_{33} of these ceramics was measured using a piezo-d_{33} meter (ZJ-3A, China). An impedance analyzer (Solartron Gain Phase Analyzer) was employed to characterize their dielectric properties. The dielectric behavior as a function of temperature was obtained using an *LCR* meter (HP 4980, Agilent, USA). Ferroelectric properties of these ceramics were studied by using the Radiant precise workstation (Radiant Technologies, Medina, NY).

3. Results and discussion

Fig. 1(a) plots the XRD patterns of $(Ba_{0.85}Ca_{0.15})(Ti_{1-x}Zr_x)O_3$ ceramics as a function of Zr content. All ceramics are of a perovskite crystal structure, and the secondary phases cannot be observed in the range detected. To clearly analyze the phase structure of all ceramics, the enlarged XRD patterns in the range of 2θ from 45° to 46.5° for all ceramics were shown in Fig. 1(b). The diffraction peak positions of these ceramics are shifted to a lower angle with the increase of Zr content, because the ionic radius (0.087 nm) of Zr^{4+} is larger than that (0.068 nm) of Ti^{4+}. The (2 0 0) and (0 0 2) diffraction peaks of BCTZ ceramics gradually merge with increasing the Zr content, confirming an involvement of a phase transition. The BCTZ ceramic at $x = 0$ is of a tetragonal phase, where the {2 0 0}-reflections (at 45–46.5°) associated with tetragonality show unique splitting.[20,21] With increasing the Zr content ($x < 0.10$), the symmetry of the ceramics was identified as rhombohedral phase.[22] The interval between (2 0 0) and (0 0 2) reflections also gradually becomes smaller, indicating the coexistence of tetragonal and rhombohedral phases. The cubic phase appears and increases continuously with further increasing the Zr content ($x \geq 0.10$),[23] where their (2 0 0) and (0 0 2) diffraction peaks almost emerge together. Therefore, the coexistence of tetragonal and rhombohedral phases is formed for the BCTZ ceramic with $x = 0.10$ at near room temperature.

The Raman spectra in the region of 200–1000 cm^{-1} at room temperature is characterized for further confirming the phase evolution of BCTZ ceramics, as plotted in Fig. 2(a). The modes split into the longitudinal (LO) and transverse (TO) components due to the long electrostatic force associated with the lattice ionicity induced by Ba21 ions in BCTZ, and have been represented for the $(Ba,Ca)(Zr,Ti)O_3$ lattice.[24] The Raman modes of $BaTiO_3$-based materials are mainly assigned to be $A_1(TO_1)$, $A_1(TO_2)$, $E(TO_2)$, $A_1(TO_3)$, and $A_1(LO_3)/E(LO_3)$. The $E(TO_2)$ phonon mode often confirms the existence of the tetragonal crystalline structure in $BaTiO_3$-based materials.[25] In the present work, the peak intensities of

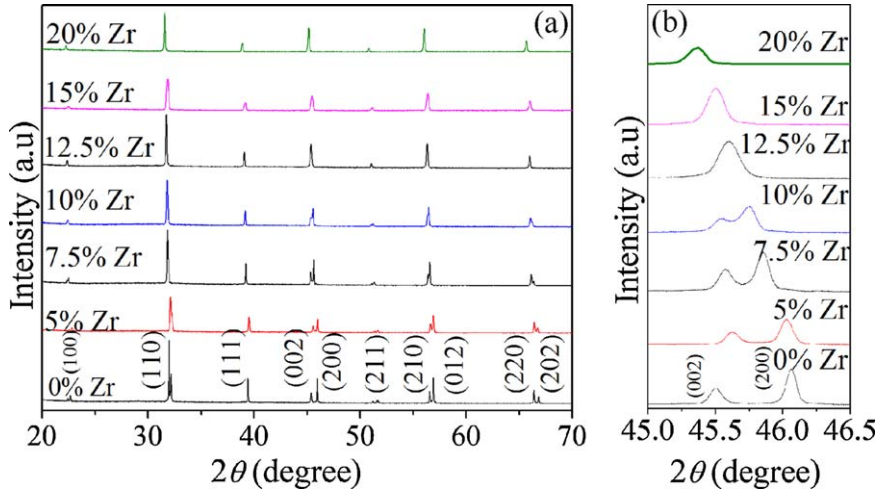

Fig. 1. (a) XRD patterns and (b) enlarged XRD patterns in the 2θ range of 45–46.5° of $(Ba_{0.85}Ca_{0.15})(Ti_{1-x}Zr_x)O_3$ ceramics.

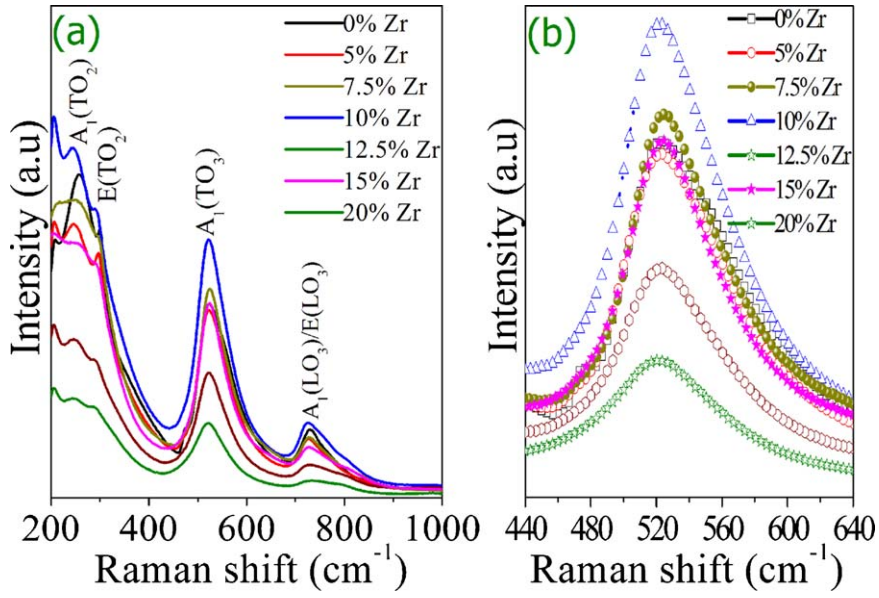

Fig. 2. (a) Raman spectrum and (b) expanded Raman spectrum of $(Ba_{0.85}Ca_{0.15})(Ti_{1-x}Zr_x)O_3$ ceramics.

the $E(TO_2)$ mode become weaker with an increase in Zr content, that is, the splitting of the $A1(TO_2)$ mode decreases, confirming the involvement of a structural disorder and a structural phase transition from the tetragonal state induced by the Zr substitution for the Ti site in $(Ba_{0.85}Ca_{0.15})(Ti_{1-x}Zr_x)O_3$.[26] Fig. 2(b) shows the expanded Raman spectrum of $(Ba_{0.85}Ca_{0.15})(Ti_{1-x}Zr_x)O_3$ ceramics. There is an obvious difference in their Raman shifts with increasing the Zr content. The vibration in Raman patterns has a broadening effect, indicating that the structure disorder results from the Zr substitution for the Ti site besides the lattice distortion. The XRD patterns and Raman spectrum show that the abnormal phenomenon appears for the ceramic with $x = 0.10$, confirming the involvement of a phase transition in such a ceramic system. Similar phenomenon has been also observed in the $Na_{0.5}Bi_{0.5}TiO_3$–$BaTiO_3$ ceramic system.[27] Therefore, the micro-Raman scattering spectra further conforms the existence of a phase transition in these ceramics.

Fig. 3 shows the temperature dependence of phase structures for the $(Ba_{0.85}Ca_{0.15})(Ti_{1-x}Zr_x)O_3$ ceramics with different Zr contents, measured by the high temperature XRD. The phase evolution is demonstrated for all BCTZ ceramics, and the tetragonal-cubic phase transition temperature of BCTZ ceramics decreases with an increase in Zr content. Therefore, it can be concluded that the phase structure of BCTZ ceramics transforms from a tetragonal phase to a cubic phase with an increase in measurement temperatures according to these characteristic peaks, and the decrease in Curie temperature is attributed to an increase in Zr content.[28]

Fig. 4(a)–(f) shows the surface morphologies of $(Ba_{0.85}Ca_{0.15})(Ti_{1-x}Zr_x)O_3$ ceramics with $x = 0$, 0.05, 0.075, 0.10, 0.15, and 0.20, respectively. With the increase of Zr content, the $(Ba_{0.85}Ca_{0.15})(Ti_{1-x}Zr_x)O_3$ ceramics become much denser, and their average grain size gradually increases, as shown in Fig. 5. Huang et al.[22] and Dixit et al.[29] have reported that the morphology of $Ba(Zr,Ti)O_3$ materials is

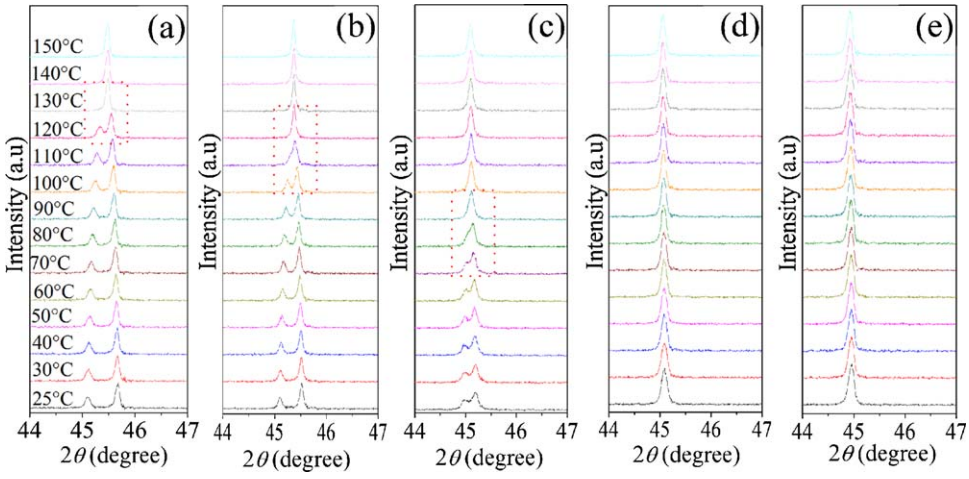

Fig. 3. Temperature dependence of XRD patterns for the $(Ba_{0.85}Ca_{0.15})(Ti_{1-x}Zr_x)O_3$ ceramics: (a) $x = 0$, (b) $x = 0.05$, (c) $x = 0.10$, (d) $x = 0.15$, and (e) $x = 0.20$.

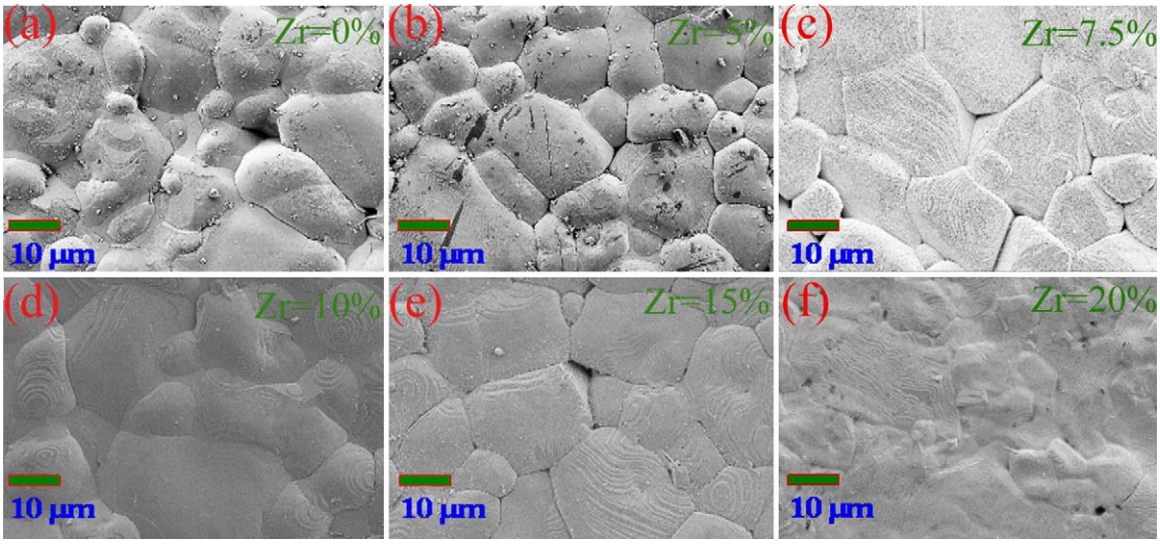

Fig. 4. Surface morphologies of $(Ba_{0.85}Ca_{0.15})(Ti_{1-x}Zr_x)O_3$ ceramics: (a) $x=0$, (b) $x=0.05$, (c) $x=0.075$, (d) $x=0.10$, (e) $x=0.15$, and (f) $x=0.20$.

strongly dependent on the Zr content, and the Zr substitution helps improve the grain growth of these materials. The content of the cubic phase gradually increases with increasing the Zr content,[23] and thus the morphological evolution with Zr contents in present work may be attributed to the increase of a cubic phase in these ceramics.[29] In order to further characterize the effect of Zr content on the density of all ceramics in this work, we measured their relative density, as shown in Fig. 5. The relative density of the ceramics increases with increasing the Zr content from $x=0$–0.09, and then slightly increases with further increasing the Zr content for the ceramics with $x>0.09$. Therefore, the introduction of Zr plays an important role in the improvement of the density of $BaTiO_3$-based ceramics.

Fig. 6 plots the temperature dependence of the dielectric behavior for the $(Ba_{0.85}Ca_{0.15})(Ti_{1-x}Zr_x)O_3$ ceramics, measured at 1, 10, 100, and 1000 kHz. The tetragonal-cubic phase transition (T_C) is observed in these ceramics, while the coexistence of two phases cannot be clearly observed in the temperature range involved except for the ceramic with $x=0.10$. The T_C value of BCTZ ceramics is shifted to a lower temperature with increasing Zr content, which is well in agreement with the temperature dependence of XRD patterns in Fig. 3. The formation of the coexistence of two phases locating at near room temperature usually benefits to the improvement in the piezoelectric properties of $BaTiO_3$-based ceramics.[7] In addition, all ceramics possess a low dielectric loss in the present work, and the peaks of the dielectric constant vs. temperature become much broader with increasing the Zr content.

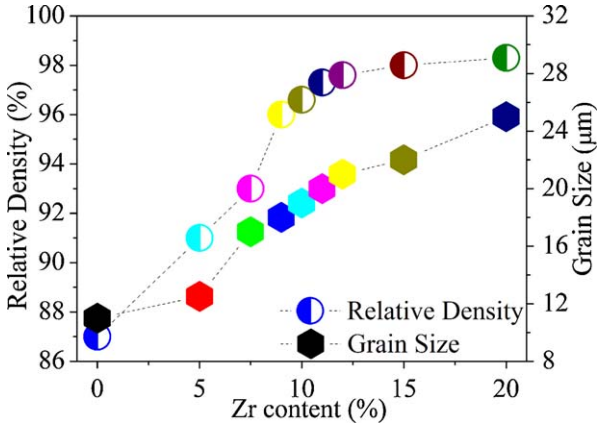

Fig. 5. Relative density and grain size of $(Ba_{0.85}Ca_{0.15})(Ti_{1-x}Zr_x)O_3$ ceramics as a function of Zr contents.

Fig. 7(a) plots the T_C value of BCTZ ceramics as a function of x. The T_C values of BCTZ ceramics gradually decrease from ~406 K to ~339 K with the increase of Zr content, due to the introduction of Zr.[28] Fig. 7(b) shows the temperature dependence of the dielectric constant of BCTZ ceramics at the measurement frequency of 1 kHz. The $(Ba_{0.85}Ca_{0.15})(Ti_{0.90}Zr_{0.10})O_3$ ceramic locating at the existence of two phases has a highest permittivity peak than those of ceramics with other compositions.[7]

Fig. 8(a) shows the dielectric properties of $(Ba_{0.85}Ca_{0.15})(Ti_{1-x}Zr_x)O_3$ ceramics in the frequency range of 10^1–10^6 Hz. The dielectric constant (ε_r) of all ceramics slightly changes in the range of measurement frequencies, while the dielectric loss ($\tan\delta$) of all ceramics exhibits obviously different. The increase in ε_r at high frequencies appears to be an instrumental artifact associated with the LCR resonance. Fig. 8(b) plots the ε_r and $\tan\delta$ values at 1 kHz as a function of Zr content for $(Ba_{0.85}Ca_{0.15})(Ti_{1-x}Zr_x)O_3$ ceramics. The ε_r values of BCTZ ceramics increase with increasing the Zr content, while the $\tan\delta$ values decrease quickly at $x\leq 0.10$, and almost keep unchanged at $x>0.10$. Fig. 8(c) shows the P–E loops of BCTZ ceramics with varying Zr contents. The ferroelectric properties strongly depend on the Zr content in BCTZ ceramics. Fig. 8(d) plots the $2P_r$ and $2E_c$ values as a function of Zr content in $(Ba_{0.85}Ca_{0.15})(Ti_{1-x}Zr_x)O_3$ ceramics. The remnant polarization ($2P_r$) increases gradually, reaches a maximum value at $x=0.10$, and then decreases with further increasing the Zr content. This result confirms that the BCTZ ceramics with the coexistence of two phases at

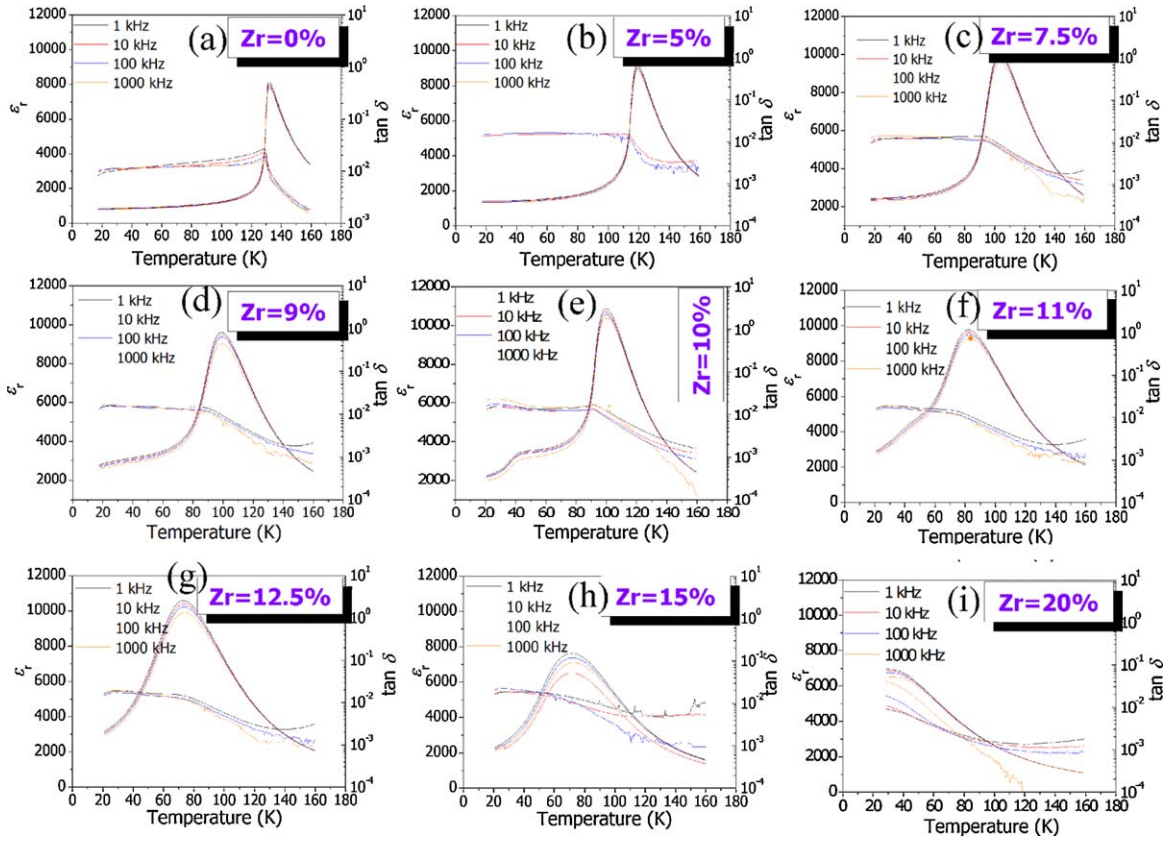

Fig. 6. Temperature dependence of the dielectric behavior of $(Ba_{0.85}Ca_{0.15})(Ti_{1-x}Zr_x)O_3$ ceramics: (a) $x=0$, (b) $x=0.05$, (c) $x=0.075$, (d) $x=0.09$, (e) $x=0.10$, (f) $x=0.11$, (g) $x=0.125$, (h) $x=0.15$, and (i) $x=0.20$.

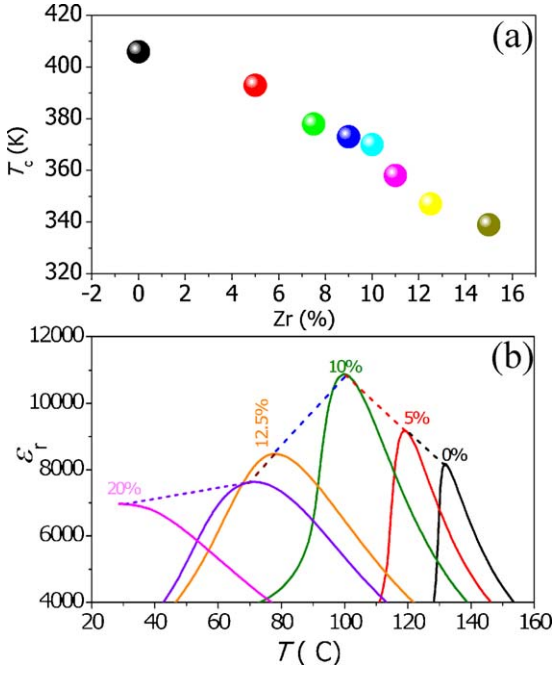

Fig. 7. (a) T_C values of $(Ba_{0.85}Ca_{0.15})(Ti_{1-x}Zr_x)O_3$ ceramics as a function of Zr content. (b) Highest permittivity peak appears of $(Ba_{0.85}Ca_{0.15})(Ti_{1-x}Zr_x)O_3$ ceramics as a function of Zr content.

near room temperature have a higher $2P_r$ value than those of the ceramics with other compositions. However, their $2E_c$ values decrease with increasing the Zr content. The ceramic with $x=0.10$ has a low coercive field of $2E_c \sim 0.47$ kV/mm, indicating that the ceramic is very "soft" with respect to the electric field because the free energy profile of polarization rotation is anisotropically flattened at this phase boundary.[7]

Fig. 9(a) plots the electrical properties of BCTZ ceramics as a function of Zr content. The maximum d_{33} and k_p values are located for the ceramic with $x=10\%$, which is induced by the coexistence of two phases at near room temperature. This implies that the proximity of the phase transition temperature to near room temperature plays more important roles in enhancing piezoelectric properties of BCTZ ceramics, while the Q_m values for all ceramics are in the range of 59–161. Subsequently, we investigate the effect of the poling condition on the electrical properties of the BCTZ ceramic with $x=0.10$. Fig. 9(b) shows the piezoelectric properties of the BCTZ ceramic with $x=0.10$ as a function of the poling temperature (T_p), where the d_{33} value in this work is an average value by measuring at least five samples. The ceramic is poled under the condition of the poling time of 30 min and the poling electric field of 3 kV/mm at different T_p values. The T_p value has obviously influenced the piezoelectric properties of BCTZ ceramics in the present work. Better piezoelectric properties have been demonstrated for the ceramic with $x=0.10$ by using the $T_p \sim 20$–$60\,^{\circ}C$, which is close to the

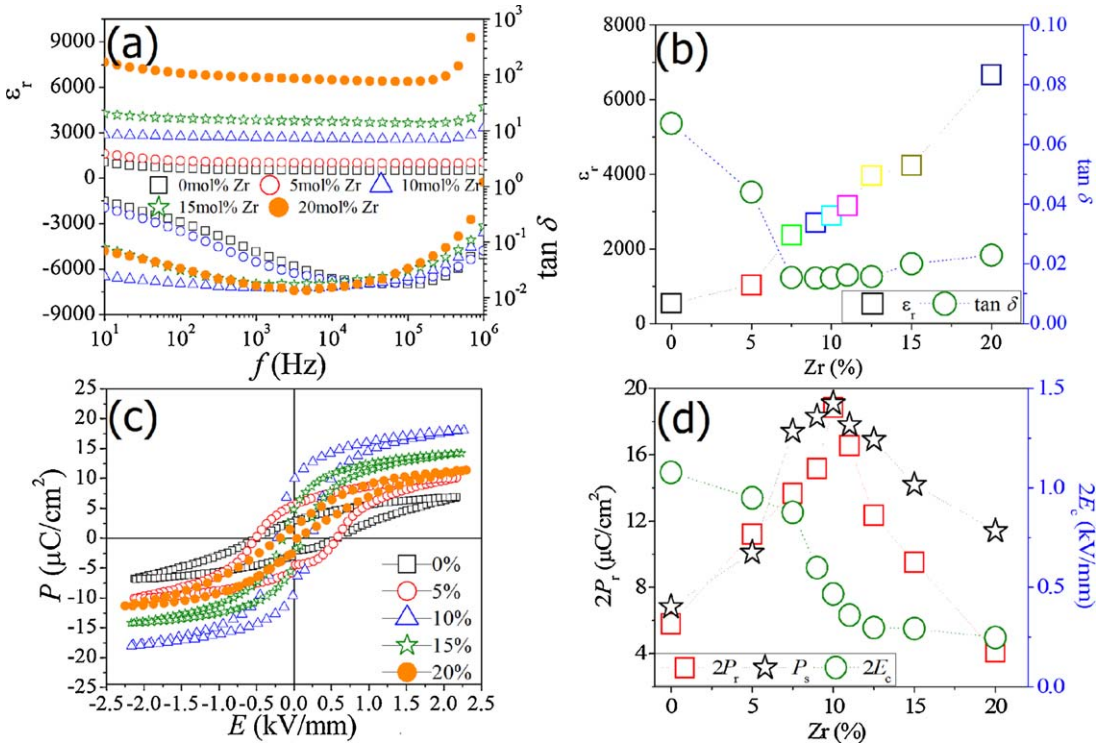

Fig. 8. (a) Dielectric properties vs. frequencies, (b) ε_r and tan δ values at 1 kHz as a function of Zr content, (c) P–E loops, and (d) $2P_r$ and $2E_c$ values as a function of Zr content of $(Ba_{0.85}Ca_{0.15})(Ti_{1-x}Zr_x)O_3$ ceramics.

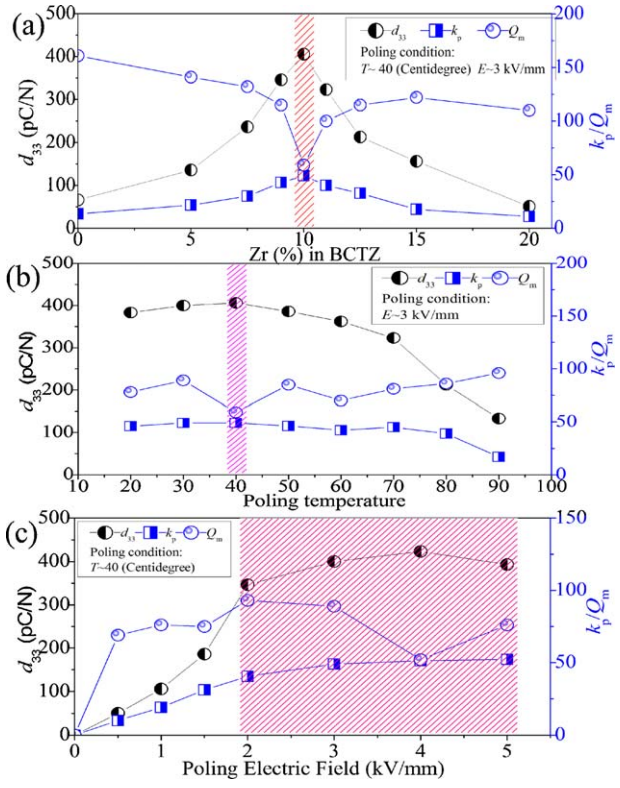

Fig. 9. (a) d_{33}, k_p, Q_m vs. Zr content for the $(Ba_{0.85}Ca_{0.15})(Ti_{1-x}Zr_x)O_3$ ceramics, (b) d_{33}, k_p, Q_m vs. poling temperature for the $(Ba_{0.85}Ca_{0.15})(Ti_{0.90}Zr_{0.10})O_3$ ceramic, and (c) d_{33}, k_p, Q_m vs. poling electric field for the $(Ba_{0.85}Ca_{0.15})(Ti_{0.90}Zr_{0.10})O_3$ ceramic.

phase transition temperature of two phases in such a ceramic in Fig. 6. This phenomenon should be because the volume fractions of domains are much easier to be switched during poling for the ceramic with the coexistence of two phases when the T_p value is close to MPB. Therefore, it can be concluded that the optimum T_p value of these ceramics enhances the piezoelectric properties of BCTZ ceramics in this work. Fig. 10(c) plots the electrical properties vs. poling electric fields (E) for the ceramic with $x = 0.10$, where the poling temperature is 40 °C. Its d_{33} value dramatically increases at $E < 2$ kV/mm, and then almost keeps unchanged with the further increasing E. Poor piezoelectric properties of the ceramic poled at $E < 2$ kV/mm is due to the incompletely switching of domains in BCTZ ceramics.

Fig. 10(a) plots the phase angle (θ) and the d_{33} values vs. Zr content of $(Ba_{0.85}Ca_{0.15})(Ti_{1-x}Zr_x)O_3$ ceramics. The θ value of the BCTZ ceramic with $x = 0.05$ is low (~47.8°), reaches a maximum (~79.0°) with increasing Zr content, and then decreases with further increasing Zr content (~55.0°), confirming that a more square-like resonance is demonstrated for the ceramic with $x = 0.10$. In the present work, the θ value is correlated to the d_{33} value for these BCTZ ceramics with different Zr content, that is, a higher θ value is corresponding to a larger d_{33} value. In this paper, the $(Ba_{0.85}Ca_{0.15})(Ti_{0.90}Zr_{0.10})O_3$ ceramic with a highest θ value of ~79° has a largest d_{33} value of ~406 pC/N, where the sample is poled at $E \sim 3$ kV/mm and $T_p \sim 40$ °C. Therefore, a higher d_{33} value is demonstrated for the $(Ba_{0.85}Ca_{0.15})(Ti_{0.90}Zr_{0.10})O_3$ ceramic with a higher θ value because the $(Ba_{0.85}Ca_{0.15})(Ti_{0.90}Zr_{0.10})O_3$ ceramic is located at near the coexistence of two phases. The insert in Fig. 10(a) plots the frequency dependence of the impedance (Z) and phase

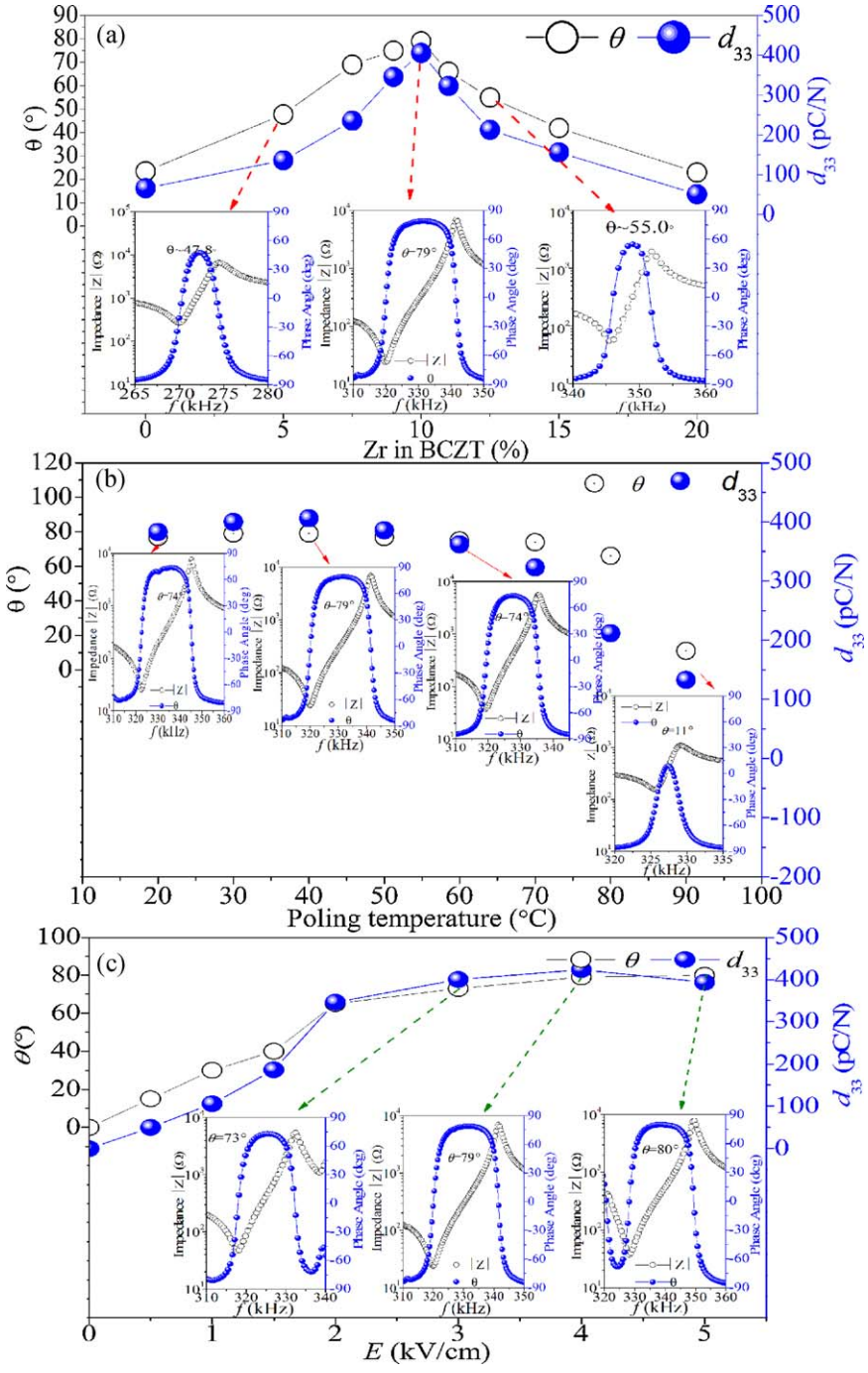

Fig. 10. (a) θ and d_{33} vs. Zr content of BCTZ ceramics; (b) θ and d_{33} vs. poling temperature of $(Ba_{0.85}Ca_{0.15})(Ti_{0.90}Zr_{0.10})O_3$ ceramics; (c) θ and d_{33} vs. poling electric fields of $(Ba_{0.85}Ca_{0.15})(Ti_{0.90}Zr_{0.10})O_3$ ceramics. Where the inserts are frequency dependence of the impedance (Z) and θ of $(Ba_{0.85}Ca_{0.15})(Ti_{1-x}Zr_x)O_3$ ceramics.

angle (θ) of $(Ba_{0.85}Ca_{0.15})(Ti_{1-x}Zr_x)O_3$ ceramics. This result well indicates the change of θ value with Zr composition. Fig. 10(b) plots the θ and d_{33} values vs. the poling temperature of $(Ba_{0.85}Ca_{0.15})(Ti_{0.90}Zr_{0.10})O_3$ ceramics. The θ value decreases with the increase of the poling temperature, and a slightly highest θ value is observed at $T_p = 40\,^{\circ}C$, as confirmed by the frequency dependence of the Z and θ in the insert of Fig. 10(b). Similar to the change of θ values, a largest d_{33} value is also obtained at $T_p = 40\,^{\circ}C$. Therefore, the θ value for the same material as a function of T_p can well evaluate its piezoelectric constant. Fig. 10(c) plots the θ and d_{33} values vs. the poling electric field of $(Ba_{0.85}Ca_{0.15})(Ti_{0.90}Zr_{0.10})O_3$ ceramics. A better d_{33} value can be obtained for $E > 2$ kV/mm, and a lower E value ($E < 2$ kV/mm) degrades its piezoelectric properties of $(Ba_{0.85}Ca_{0.15})(Ti_{0.90}Zr_{0.10})O_3$ ceramics because of a low θ value induced by the incompletely poling state, as shown in the insert of Fig. 10(c). Therefore, the effect of the poling condition on the piezoelectric constant of BCTZ

ceramics is well evaluated by the θ value in the present work.[30–33]

4. Conclusions

$(Ba_{0.95}Ca_{0.05})(Ti_{1-x}Zr_x)O_3$ lead-free piezoelectric ceramics were fabricated by the solid-state reaction method, and sintered at 1500 °C for 2 h in air atmosphere. The coexistence of tetragonal and rhombohedral phases is identified for the BCTZ ceramic at $x \sim 0.10$, confirmed by the XRD patterns, the Raman spectroscopy, and the temperature dependence of the dielectric behavior. Enhanced electrical properties are demonstrated for the BCTZ ceramics by optimizing the composition and the poling condition. The BCTZ ceramic near this phase transition has excellent electrical properties: $d_{33} \sim 423$ pC/N, $k_p \sim 51.2\%$, $2P_r \sim 18.86\ \mu C/cm^2$, $2E_c \sim 0.47$ kV/mm, $\varepsilon_r \sim 2892$, and $\tan\delta \sim 1.53\%$. The present study demonstrates that (Ba,Ca)(Ti,Zr)O_3 ceramics are a promising candidate for the lead-free piezoelectric ceramics.

Acknowledgements

Dr. Jiagang Wu gratefully acknowledges the supports of the introduction of talent start funds of Sichuan University (2082204144033), the National Science Foundation of China (NSFC Nos. 51102173, 50772068 and 50972001), and the National University of Singapore.

References

1. Saito Y, Takao H, Tani T, Nonoyama T, Takatori K, Homma T, et al. *Nature* 2004;**432**:84.
2. Rödel J, Jo W, Seifert KTP, Anton EM, Granzow T, Damjanovic D. *J Am Ceram Soc* 2009;**92**:1153.
3. Xiao DQ, Wu JG, Wu L, Zhu JG, Yu P, Lin DM, et al. *J Mater Sci* 2009;**44**:5408.
4. Zhang SJ, Xia R, Shrout TR. *J Electroceram* 2007;**19**:251.
5. Wu JG, Wang YY, Xiao DQ, Zhu JG. *Appl Phys Lett* 2007;**91**:132914.
6. Wu JG, Xiao DQ, Wang YY, Zhu JG, Wu L, Jiang YH. *Appl Phys Lett* 2007;**91**:252907.
7. Liu WF, Ren XB. *Phys Rev Lett* 2009;**103**:257602.
8. Bao H, Zhou C, Xue D, Gao J, Ren X. *J Phys D: Appl Phys* 2010;**43**:465401.
9. Xue D, Zhou Y, Bao H, Zhou C, Gao J, Ren X. *J Appl Phys* 2011;**109**:054110.
10. Damjanovic D. *Appl Phys Lett* 2010;**97**:062906.
11. Damjanovic D, Klein N, Li J, Porokhonskyy V. *Funct Mater Lett* 2010;**3**:5.
12. Zhang JX, Xiang B, He Q, Seidel J, Zeches RJ, Yu P, et al. *Nat Nanotechnol* 2011;**6**:93.
13. Zuo RZ, Fang XS, Ye C. *Appl Phys Lett* 2007;**90**:092904.
14. Li E, Kakemoto H, Wada S, Tsurumi T. *J Ceram Soc Jpn* 2007;**115**:250.
15. Zhang SJ, Xia R, Shrout TR. *Appl Phys Lett* 2007;**91**:132913.
16. Du HL, Zhou WC, Luo F, Zhu DM, Qu SB, Pei ZB. *Appl Phys Lett* 2007;**91**:202907.
17. Fu HX, Cohen RE. *Nature (London)* 2000;**403**:28.
18. Damjanovic D. *J Am Ceram Soc* 2005;**88**:2663.
19. Bellaiche L, Garcia A, Vanderbilt D. *Phys Rev Lett* 2000;**84**:5427.
20. Mitsui T, Westphal WB. *Physiol Rev* 1961;**124**:1354.
21. Fu DS, Itoh M, Koshihara S, Kosugi T, Tsuneyuki S. *Phys Rev Lett* 2008;**100**:227601.
22. Dobal PS, Dixit A, Katiyar RS, Yu Z, Guo R, Bhalla AS. *J Appl Phys* 2001;**89**:8085.
23. Huang HH, Chiu HH, Wu NC, Wang MC. *Metall Mater Trans A* 2008;**39**(13):3276.
24. Dobal PS, Katiyar RS. *J Raman Spectrosc* 2002;**33**:405.
25. Begg BD, Kim S, Finnie, Vance ER. *J Am Ceram Soc* 1996;**79**:2666.
26. Pontes FM, Escote MT, Escudeiro CC, Leite ER, Longo E, Chiquito AJ, et al. *J Appl Phys* 2004;**96**:4386.
27. Cheng HW, Zhang XJ, Zhang ST, Feng Y, Chen YF, Liu ZG, et al. *Appl Phys Lett* 2004;**85**:2319.
28. Chen H, Yang C, Fu C, Shi J, Zhang J, Leng W. *J Mater Sci* 2008;**19**:379.
29. Dixit A, Majumder SB, Dobal PS, Katiyar RS, Bhalla AS. *Thin Solid Films* 2004;**447–448**:284.
30. Fujioka C, Aoyagi R, Takeda H, Okamura S, Shiosaki T. *J Eur Ceram Soc* 2005;**25**:2723.
31. Lin D, Kwok KW, Chan HLW. *J Alloys Compd* 2008;**461**:273.
32. Park HY, Seo IT, Choi MK, Nahm S, Lee HG, Kang HW, et al. *J Appl Phys* 2008;**104**:034103.
33. Chen Q, Peng Z, Liu H, Xiao D, Zhu J, Zhu J. *J Am Ceram Soc* 2010;**93**(9):2788.